Optica Applicata, Vol. XXXVII, No. 1–2, 2007

The interferometry based on regular lattice of optical vortices

JAN MASAJADA

Institute of Physics, Wrocław University of Technology, Wybrzeże Wyspiańskiego 27, 50-370 Wrocław, Poland; e-mail: Jan.Masajada@pwr.wroc.pl

The optical vortices are point phase dislocations. The point where the phase is undetermined is called a vortex point. The lattice of optical vortices can be generated by the interference of three or more plane waves, but the optical vortex lattice generated by interference of three plane waves is regular and posses a number of special properties, which are discussed in this paper. The basic geometrical features of such a regular lattice of optical vortices are also presented. The regular lattice of optical vortices is a base for optical vortex interferometer (OVI). The OVI takes advantages of special properties of three plane wave interference field. The relations between OVI advantages and special features of the vortex lattice are discussed in brief.

Keywords: optical vortex, vortex lattice, interferometry.

1. Introduction

The wavefront carrying optical vortex has a characteristic helical wavefront. Along the axis of the helice the phase is undetermined [1, 2]. Such singular lines are stable and generic phenomenon. Optical vortices are associated with the non-zero angular momentum carrying by the wavefront they belong to. Depending on the orientation of the helice they are said to have positive or negative topological charge [1, 2]. In the plane cross-section, the line along which the phase is undetermined becomes a point – vortex point. The light beams containing optical vortices can be generated in various ways, for example, by use of synthetic holograms [1, 2], phase converter made with two cylindrical lenses [3], phase plates [3], laser mode separation [4], interference of two plane waves of non-uniform amplitude [5]. The regular lattice of optical vortices can be produced by interference of three plane waves. This fact was discussed in [6, 7] in the context of potential application to interferometry (optical vortex interferometry – OVI). In subsequent papers [8–12], the idea of OVI as well as its possible applications and methods for localization of vortex points were presented. It was also shown that by a simple calibration procedure the topological charge of vortices in the OVI interference field can be determined [13–15]. This means that in

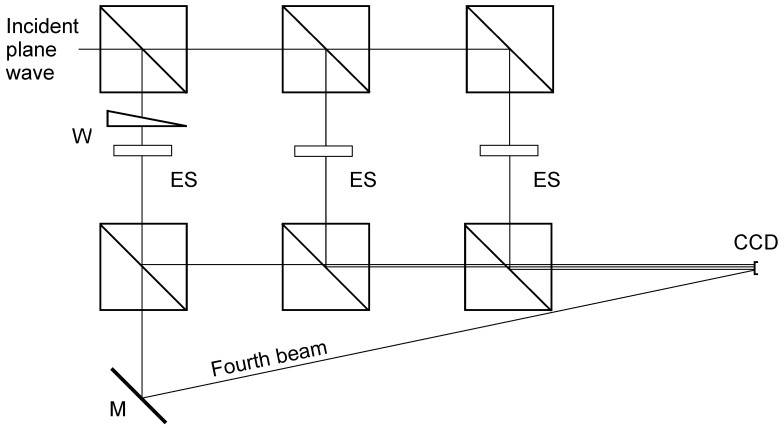

Fig. 1. Six cubic beam splitters produce a set of three plane waves A, B, C. The beams interfere and produce a regular vortex lattice. ES are electronic shutters, which enable taking the following interferograms: $A + B$, $A + C$, $B + C$, $A + B + C$. The electronic shutters are not necessary when using one frame ($A + B + C$) measurement procedure. Optical wedge W inserted into the beam A is used for OVI system testing. The fourth beam is used to proof the presence of optical vortices.

the case of OVI the phase can be reconstructed without ambiguity (phase unwrapping problem [16]). The basic optical setup of the OVI is very simple and flexible. Every optical system that brings three plane waves to interfere under small angles can be used as OVI. Figure 1 shows an example of the basic optical scheme of OVI. At the first glance the OVI seems to be a simple extension of the classical two beam interferometry, however, this is not the case. The main purpose of this paper is to show that OVI is a new instrument in a more fundamental meaning – one can speak about a new kind of interferometry, which has its own unique character.

Interferometry has been developing since the 19th century. At present, there is a huge literature concerning both theoretical and practical aspects of interferometry (see [17], for references). The multiwave interferometry is also known and well described (Fabry–Perot interferometer [18], for example). A question naturally arises: can there be anything important and special in the field produced by three interfering plane waves which was overlooked during more than hundred years of research? The answer to this question is positive and it is a subject of the present paper. The interference field generated by three plane waves has a number of special properties. The relations between special properties of such interference field and OVI advantages are discussed briefly in Section 4. In the previous papers [6–10], this problem was discussed partially. While writing those papers the authors realized that the three plane wave case is special, but the picture was not complete and the presentation was not focused on the special features of the three plane wave interference field.

The interference of three plane waves producing a regular array of vortex points has also been investigated in a different context. NICHOLLS and NYE [19] used it for

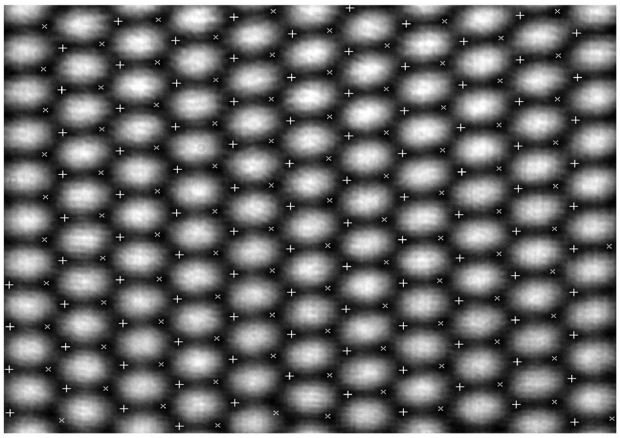

Fig. 2. The intensity distribution of the interference field obtained by three plane waves (experiment). The two groups studying the measurement potential of such interference field have focused on the two different aspects: the dark areas containing vortex points or light areas of maximum intensity. The position of vortex points is marked by pluses or crosses to distinguish between different topological charges.

studying some subtle details of the phase dislocations in the electromagnetic field. BIALYNICKI-BIRULA *et al.* [20], explored it as an example for their studies on the relativistic quantum description of the electromagnetic field. SCHONBRUN *et al.* [21] have suggested using such arrays for small particle trapping. It is interesting that at the same time a number of papers dealing with the interference of three or more plane waves, but focused on the array of bright spot (Fig. 2) were published. The authors of those papers considered the metrological applications of such array of spots [22–27], microlens array manufacturing [28] and 2-D photonic crystals manufacturing [29]. Studying the reference lists of the papers published by both groups, *i.e.*, the group focused on the vortex points and the group focused on the bright spots, one can conclude that they did not know about each other. This seems to be the first paper that contains references covering both bright and dark side of the multi-plane wave interference field.

2. Three plane waves interference field

2.1. Definitions and basic geometrical characteristics

In classical interferometry the phase singularities are considered as a source of problems. The regions containing phase singularities are either neglected in data processing or treated in a special way [16, 30, 31]. In this context, the OVI goes into opposite direction. A number of optical vortices are generated within the interference field and the vortex points are the points where the interference field is analyzed. The new instrument brings about new possibilities but requires new methods. For example, the methodology for data processing which is used for classical

interferometry can support the measurements with OVI, but basically new approach is necessary. In this section, the new definitions and basic properties of vortex lattice are presented. They are both new (uncommon in the standard interferometry) and useful when working with the OVI.

As was mentioned above the regular lattice of OVI can be generated by the interference of three plane waves, here denoted by A, B, C. At every point, the resulting interference field can be represented by three phasors as discussed in [6–8]. The length of phasor represents the wave amplitude and its orientation angle represents the wave phase. The phasors corresponding to waves A, B, C are denoted by **a**, **b**, **c**, respectively. Since, at the vortex point the light amplitude is equal to zero [1, 2], the **a**, **b**, **c** phasors form a triangle.

The interference field of n-plane waves can be transformed to the case where one of the interfering waves has constant phase over the whole observation plane and the vortex points preserve their positions. Thus, such a transformation preserves vortex lattice geometry, but the local phase portrait of the interference field is changed. This transformation is named constant-lattice transformation (CLT) and is discussed in [6, 7]. The CLT results in unphysical set of waves and as such should be treated as purely technical step. In this paper, the CLT is used for transforming the interfering waves to a configuration where the wave marked as A has constant phase over the observation plane. Such a transformation is given by the formulas:

$$\begin{aligned} k'_{xQ} &= k_{xQ} - k_{xA} \\ k'_{yQ} &= k_{yQ} - k_{yA} \\ k'_{zQ} &= k_{zQ} - k_{zA} \end{aligned} \tag{1}$$

where $k_{\nu Q}$ is the ν-coordinate of the wavevector of wave Q, while $\nu \in (x, y, z)$ and $Q \in (A, B, C, D, E, \ldots)$; here indices A, B, C, D, E, ... denote different plane waves and A', B', C', D', E', ... denote the transformed waves.

The constant angle line (CAL) of two waves, in the observation plane, is a line along which the phase angle between these waves is constant (Fig. 3). The CALs of the given two plane waves are mutually parallel. The value of the CAL of two waves is the value of the corresponding phase angle between these waves. The pattern formed by CALs is periodic. Obviously, in the case of plane waves having uniform amplitude the CALs are parallel to the interference fringes of these waves, however, it is more convenient to use CALs instead of interference fringes while analyzing the measurements performed with OVI. The question of CALs period needs more attention. Since, in the case of the interference field produced by two beams there is no way one can distinguish between the relative phase value (between two waves) α and $2\pi - 2\alpha$, the CALs period could be defined as π. However, having the vortex lattice generated by three waves, the following convention can be used: a given CAL value of two waves B and C with respect to the third wave (wave A in this paper)

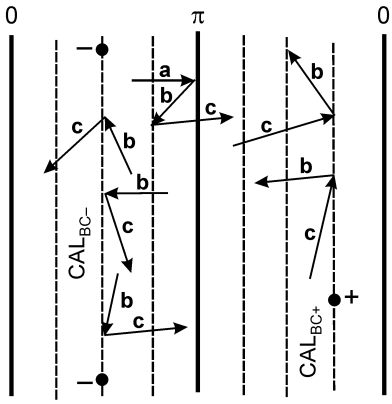

Fig. 3. A set of CALs (dashed lines) of two interfering waves *B* and *C* (see Fig. 1). The CALs are mutually parallel. By adding the third wave – wave *A* – vortex lattice is generated. The vortex points of the given topological charge lie on the CALs having the same value. Consequently, the whole pattern can be divided into two kinds of subsequently appearing regions: the regions which surround the CALs passing through the positive vortices and the negative vortices, respectively. The CALs of value 0 and π (bold lines) are the borders between these two regions. Vortex points are marked by black circles. Their sign is marked by small + or –. The arrows plotted with bold line represent the **b** and **c** phasors. While going along the CAL, the angle between phasors **b** and **c** is constant and the phasors rotate simultaneously. The example of three part broken line, which is formed by three phasors **a**, **b**, **c** is also shown.

belongs to the interval (0, π) if this CAL lies in the region of positive vortex lattice, otherwise it belongs to the interval (π, 2π) – Fig. 3. The CALs having value 0 and π are special because phasors **a**, **b**, **c** cannot form a triangle (phasors **b** and **c** are collinear or anti-collinear (Fig. 3)). Since one can determine the vortex point topological charge [13–15], this definition is of practical value.

The normalized vector $\mathbf{K}(K_x, K_y)$ for the given wave pair is parallel to the CALs of these waves and shows the direction along which the corresponding phasors rotate anticlockwise. The vector **K** can be expressed as follows:

$$K_x = \operatorname{sign}\left[\frac{k_{yCB}}{k_{xB}k_{yC} - k_{yB}k_{xC}}\right]\frac{|k_{yCB}|}{\sqrt{k_{xCB}^2 + k_{yCB}^2}} \tag{2a}$$

$$K_y = \operatorname{sign}\left[\frac{k_{xCB}}{k_{xB}k_{yC} - k_{yB}k_{xC}}\right]\frac{|k_{xCB}|}{\sqrt{k_{xCB}^2 + k_{yCB}^2}} \tag{2b}$$

where $k_{xCB} = k_{xC} - k_{xB}$ and $k_{yCB} = k_{yC} - k_{yB}$. It is convenient to use a smart coordinate system when analyzing the OVI interference field.

It is assumed that *y*-axis of the smart coordinate system is parallel to the CALs of two waves (chosen from among three), which are mostly the reference waves in the measurements performed with OVI. It is also assumed that the *z*-axis of any

coordinate system used in this paper is perpendicular to the observation plane. In the smart coordinate system the vector **K** has coordinates:

$$K_x = 0, \quad K_y = 1 \tag{3}$$

The important fact is that the smart coordinate system is the most natural choice for data analysis when determining the vortex lattice from the experimental data.

The normalized vector $\mathbf{M}(M_x, M_y)$ is perpendicular to the vector **K**. The following convention is adopted: if one looks perpendicularly to the observation plane and at direction of light propagation (*i.e.*, along the *z*-axis of the coordinate system) the vector **M** must rotate clockwise through an angle $\pi/2$ to be parallel to vector **K**. Using this convention the coordinates of vector **M** are:

$$M_x = -K_y, \quad M_y = K_x \tag{4}$$

2.2. Vortex points handedness

Due to phase circulation the optical vortices can be classified into two categories. They are told to have positive or negative topological charge [1, 2]. It is convenient to split the vortex lattice into two sublattices, which consist of positive and negative vortices. In many cases, when talking about the negative vortex sublattice one does not mean that the lattice consists of negative vortices, but this is the way of distinguishing between the two possible cases. However, if necessary, the vortices charge can be precisely determined. In [13–15], two experimental methods for topological charge determination of vortex points are described. Although these experimental methods can be adopted for theoretical analysis it is convenient to introduce a new method. Figure 4 shows two possible triangles formed with phasors **a**, **b**, **c** at the vortex points. It is assumed that the coordinates of the wavevectors of the interfering waves are

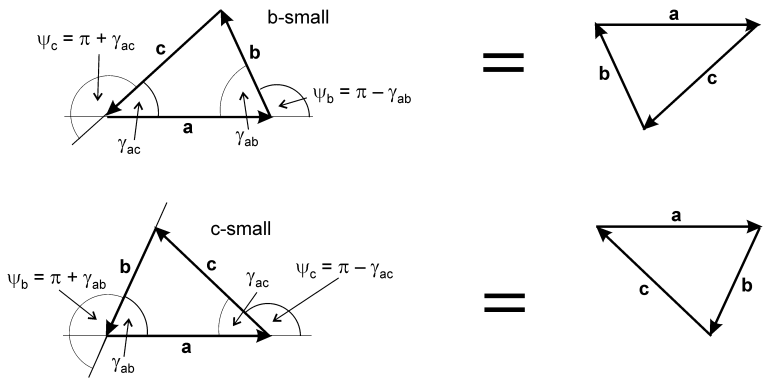

Fig. 4. Two triangles which are formed by phasors of interfering waves. They are related to two topological charges of optical vortices. The phasors which are at a smaller angle with vector **a**, are marked as b-small or c-small, respectively. The figure also shows the way of denoting the triangle angles.

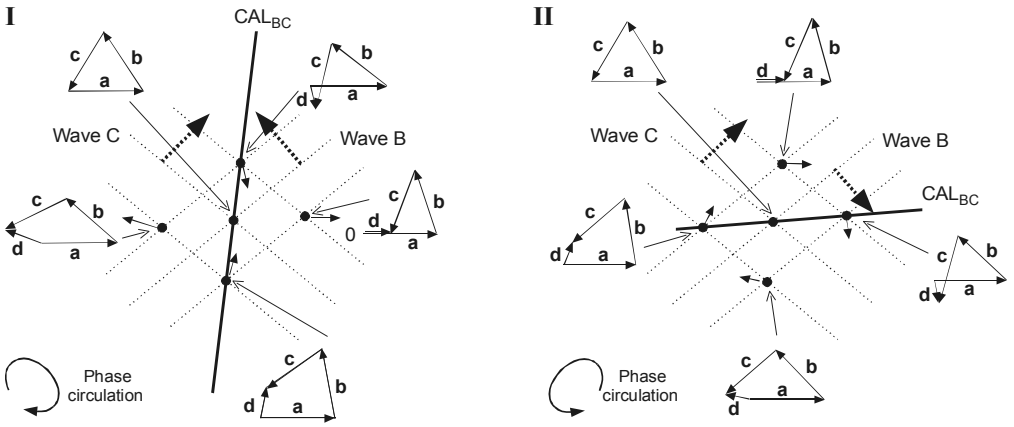

Fig. 5. The graphical way of proving the methodology for vortex sign determination. Parts **I** and **II** shows two different cases out of eight to be considered for the full analysis. The thin dotted lines are the equiphase lines of waves *B* and *C*. The wave *A* is assumed to be parallel to the observation plane, so its phase is constant (the general case can be transformed to this one by CLT). The arrows plotted with dashed lines show the direction in which the phases of waves *B* and *C* increase. The interference of waves *A*, *B*, *C* is represented by adding graphically phasors **a**, **b**, **c**. These resulting phasors at the points neighboring the given vortex points are denoted by **d**. By tracing the direction in which phasor **d** rotates while going around the vortex point one can determine the vortex charge. The CALs of waves *B* and *C* going through vortex point are plotted as bold lines.

recomputed to smart coordinate system and the coordinate system is left oriented. It is also assumed that the angles of the phasors **b** and **c** are measured against phasor **a** as shown in Fig. 4. In further considerations it does not matter, which phasor is marked as **a** or **b** or **c**. When the waves are defined by their complex amplitudes one can easily determine which vector, **b** or **c,** is at a small angle with vector **a**. The following statement can be prooved: if the wave, whose phasor is at a small angle with phasor **a** has negative *x*-coordinate of its wavevector, then the sign of the vortex point under investigation is negative (the phase circulates clockwise), otherwise it is positive (the phase circulates anticlockwise). Figure 5 gives some idea of the way the above rule has been derived. It is enough to find the topological charge of one vortex point at the observation plane. Then using the sign theorem [32], one can easily determine the topological charge of all other vortex points.

2.3. Positions of vortex points

The positions of vortex points can be uniquely determined with the use of CALs. In order to do this, the arrangement of three plane waves must be transformed by CLT in such a way that one of the three waves (named *A*) has constant phase over the observation plane. Since the transformed waves *B′* and *C′* have different relative phase at positive and negative vortex points these two sublattices should be

considered separately, however, here positive or negative may be treated just as labels. For the positive vortex points, the phase difference between interfering waves is:

$$x\,k'_{xB} + y\,k'_{yB} + \delta_B - \delta_A = \pi - \gamma_{ab} + 2\pi l \tag{5a}$$

$$x\,k'_{xC} + y\,k'_{yC} + \delta_C - \delta_A = \pi + \gamma_{ac} + 2\pi m \tag{5b}$$

$$xk_{xCB} + yk_{yCB} + \delta_C - \delta_B = \pi - \gamma_{bc} + 2\pi n \tag{5c}$$

For the negative vortex points, the phase difference between interfering waves is:

$$x\,k'_{xB} + y\,k'_{yB} + \delta_B - \delta_A = \pi + \gamma_{ab} + 2\pi l \tag{6a}$$

$$x\,k'_{xC} + y\,k'_{yC} + \delta_C - \delta_A = \pi - \gamma_{ac} + 2\pi m \tag{6b}$$

$$xk_{xCB} + yk_{yCB} + \delta_C - \delta_B = \gamma_{bc} - \pi + 2\pi n \tag{6c}$$

where δ_Q is the phase of wave Q at the coordinate system origin, γ_{ab}, γ_{bc}, γ_{ac} are triangle angles as shown in Fig. 4, and k, l, m are integers.

In the above sets, two equations of three are independent, so first two equations will be proceed. By solving the above equations for y one gets:

– positive case

$$yP_{ab} = \frac{-k'_{xB}}{k'_{yB}}\,x + \frac{\delta_A - \delta_B + \pi - \gamma_{ab} + 2\pi l}{k'_{yB}} \tag{7a}$$

$$yP_{ac} = \frac{-k'_{xC}}{k'_{yC}}\,x + \frac{\delta_A - \delta_C + \pi + \gamma_{ac} + 2\pi m}{k'_{yB}} \tag{7b}$$

– negative case

$$yN_{ab} = \frac{-k'_{xB}}{k'_{yB}}\,x + \frac{\delta_A - \delta_B + \pi + \gamma_{ab} + 2\pi l}{k'_{yB}} \tag{8a}$$

$$yN_{ac} = \frac{-k'_{xC}}{k'_{yC}}\,x + \frac{\delta_A - \delta_C + \pi - \gamma_{ac} + 2\pi m}{k'_{yB}} \tag{8b}$$

As expected, formulas (7) and (8) represent a set of lines. The vortex points are in places where the above lines intersect, that is, $yP_{ab} = yP_{ac}$ for the positive case and $yN_{ab} = yN_{ac}$ for the negative case. The solution is:

$$xP = \frac{(-\delta_{AB} + \pi - \gamma_{AB} + 2\pi l)\,k'_{yC} + (\delta_{CA} - \pi - \gamma_{AC} - 2\pi m)\,k'_{yB}}{k'_{xB}\,k'_{yC} - k'_{xC}\,k'_{yB}} \tag{9a}$$

$$xN = \frac{(-\delta_{AB} + \pi + \gamma_{ab} + 2\pi l)\, k'_{yC} + (\delta_{CA} - \pi + \gamma_{ac} - 2\pi m)\, k'_{yB}}{k'_{xB}\, k'_{yC} - k'_{xC}\, k'_{yB}} \tag{9b}$$

where $\delta_{AB} = \delta_B - \delta_A$, *etc*.

By substituting (9) into (8) the formulas for y coordinates of vortex points can be derived. Since this step is easy and the resulting formulas are long they are not listed here. When placing the subsequent integer numbers m and l into formulas (9) and corresponding formulas for y-coordinates, the position of the same vortex point may be obtained many times. This happens in the case of symmetrical arrangement of wave vectors of interfering waves. When applying these formulas for plotting the distribution of vortex points a separate module for reducing such degenerate cases is useful. The formulas (7)–(9) may be reduced to the simpler form when using the special coordinate system (including the smart coordinate system).

2.4. The distance between vortex sublattices

In the previous section, the positions of vortex points within the two vortex sublattices were determined. To complete this picture the distance between two vortex sublattices should be calculated. Since each vortex point has few neighboring vortices of opposite charge, there is a problem of the proper definition of the distance between sublattices. A full analysis of this problem is complex and there are no practical reasons, so far, to present these results. At the present stage the following procedure can be used. First, the vortex lattice should be transformed using CLT. By switching from one vortex sublattice to the other the internal geometry of the triangle is changed between two possibilities shown in Fig. 4. Let the chosen vortex point have the following internal phase relations

$$\psi_b - \psi_a = \pi - \gamma_{ab} \tag{10a}$$

$$\psi_c - \psi_a = \pi + \gamma_{ac} \tag{10b}$$

In the case of theoretical analysis such vortices can be easily identified. Then the following two sets of conditions must be met:

$$k'_{xB}\Delta x + k'_{yB}\Delta y = 2\gamma_{ab} \tag{11a}$$

$$k'_{xC}\Delta x + k'_{yC}\Delta y = -2\gamma_{ac} \tag{11b}$$

or

$$k'_{xB}\Delta x + k'_{yB}\Delta y = -2(\pi - \gamma_{ab}) \tag{12a}$$

$$k'_{xC}\Delta x + k'_{yC}\Delta y = 2(\pi - \gamma_{ac}) \tag{12b}$$

Solving these equations gives:

$$\Delta x = 2\frac{k'_{yB}\gamma_{ac} + k'_{yC}\gamma_{ab}}{k'_{xB}k'_{yC} - k'_{yB}k'_{xC}} \tag{13a}$$

$$\Delta y = -2\frac{k'_{xB}\gamma_{ac} + k'_{xC}\gamma_{ab}}{k'_{xB}k'_{yC} - k'_{yB}k'_{xC}} \tag{13b}$$

or

$$\Delta x = 2\frac{(\pi - \gamma_{ab})k'_{yC} + (\pi - \gamma_{ac})k'_{yB}}{k'_{xB}k'_{yC} - k'_{yB}k'_{xC}} \tag{14a}$$

$$\Delta y = 2\frac{(\pi - \gamma_{ab})k'_{yC} + (\pi - \gamma_{ac})k'_{yB}}{k'_{xB}k'_{yC} - k'_{yB}k'_{xC}} \tag{14b}$$

The quantities Δx and Δy show the shift between vortex points, which satisfy the conditions (10). One of these two distances can be treated as a distance between vortex sublattices. In the smart coordinate system, formulas (13) and (14) become less complicated:

$$\Delta x = -2\frac{\gamma_{ab} + \gamma_{ac}}{k_{xCB}} \tag{15a}$$

$$\Delta y = 2\frac{k'_{xB}\gamma_{ac} + k'_{xC}\gamma_{ab}}{k_{xCB}k'_{yB}} \tag{15b}$$

$$\Delta x = 2\frac{2\pi - \gamma_{ab} - \gamma_{ac}}{k_{xCB}} \tag{16a}$$

$$\Delta y = 2\frac{k'_{xB}(\gamma_{ac} - \pi) + k'_{xC}(\gamma_{ab} - \pi)}{k_{xCB}k'_{yB}} \tag{16b}$$

When analyzing the experiment one has to use experimental methods for vortex charge determination to identified vortices, satisfying conditions (10). The formulas (13)–(16) show that the distance between vortex sublattices depends on both wave vectors coordinates and the wave amplitudes.

3. Special properties of vortex lattice

At the vortex point the three phasors form a triangle and the light amplitude is zero. The geometry of the phasors at vortex point is, by definition, the internal geometry of

the vortex point. The angles of any triangle are defined uniquely by the length of its sides. So, these angles can be determined (at vortex points) by knowing the amplitude of the interfering waves or equivalently the amplitude of three interference fields $A + B$, $A + C$, $B + C$, which can be determined from the corresponding three possible two beam interferograms [6, 8]. To record such interferograms the system needs shutters (Fig. 1). These facts are not true in the case of more than three interfering waves. In this way, the first special property of the OVI interference field has been identified.

It should be noted that, although at each vortex point of the given sublattices the triangles are the same, they can be positioned differently, *i.e.*, the triangles can be rotated from one vortex point to another.

Knowing the amplitudes of interfering waves the triangle angles can be determined. In this way, the values of CALs going through vortex points are determined. Because there are three different pairs of waves there are three sets of CALs representing the vortex sublattices. The vortex points are precisely at intersections of any two (of three) sets of CALs. Thus, two of the three sets of CALs determine the whole vortex sublattices, which was shown in a more formal way in the previous section (see discussion concerning equation (9)).

The equiphase lines of interfering waves give a much more complicated picture, which results from the fact that through different vortex points the equiphase lines having different values may pass. This fact has been already noticed in [19], however, the concept of CALs has not been introduced in that paper. The first special property may be formulated in the equivalent way: the vortex sublattices can be represented by the intersection points of any two (of three) sets of CALs, whose value represents the respective triangle angles.

The above conclusions could be drawn in a more general case (generalized first property). Out of vortex point the phasors of three interfering waves form open broken lines (Fig. 2). It can be easily shown that the points which represent the given broken line are distributed in regular lattice and they have their partners of opposite "charge".

Let us assume that the CALs of wave pairs A, B and A, C form U-lattice as shown in Fig. 6. The U-lattice is formed by points were the phasors **a**, **b** and **c** form the U-pattern. Obviously, there are two possible kinds of such pattern, but this analysis is limited to one of them. The CALs which go through U-points have the value $\mathrm{CAL}_{AB} = \pi/2$ (or $3/2\pi$) and $\mathrm{CAL}_{AC} = 3/2\pi$ or $(\pi/2)$. The fourth wave D can be added in such a way that its phase at U-points is equal to π. Here, it is assumed that the amplitudes of A, B, C waves are the same, however, in the case of other values the same reasoning can be used. In such a case, phasor **d** closes the U-pattern up to the square, and the U-points became the vortex points of four wave arrangement. Moreover, this sublattice is also regular in the sense that at each vortex point the same square is formed. Now, the wave D may acquire some tilt in such a way that at the chosen point P its phase is still the same. Due to this tilt the density of equiphase lines changes. Thus, at the point P the vortex is represented by the same square, but other vortex points move from their original positions. While moving they have to

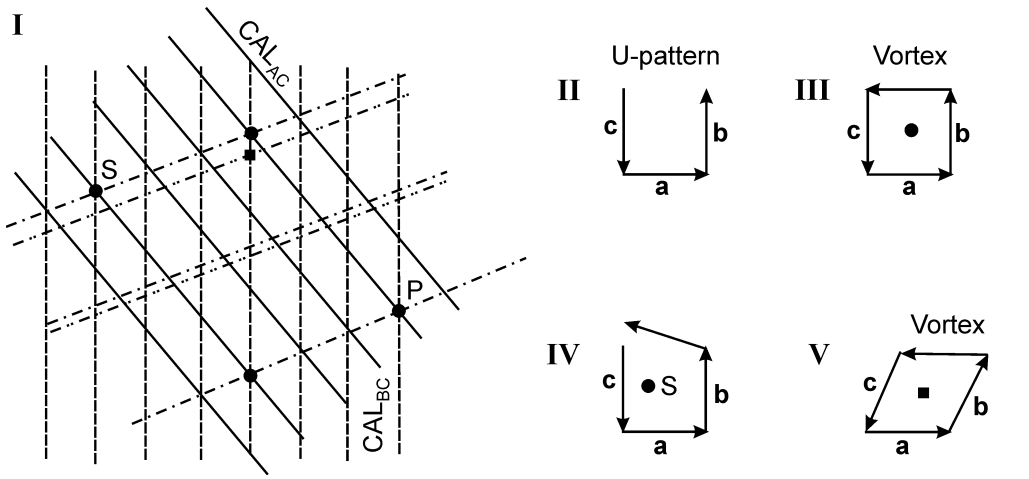

Fig. 6. Two sets of CALs of waves *A*, *C* and *B*, *C*, it is assumed that wave *A* has constant phase over the observation plane (part **I**). The *U*-points (part **II**) are distributed regularly and are marked with black circles. The equiphase lines of additional wave *D* are plotted with dash-dot line. They are fixed in such a way that at *U*-points the vortex points are born, thus the regular vortex lattice is formed (part **III**). Next the *D*-wave is tilted in such a way that their equiphase lines (dash-double dotted lines) have the same orientation but are more dense and the transformed wave *D* preserves its phase at point *P*. As a result the vortex point at *P* does not move and preserves its internal geometry (part **III**). However, the other vortex points move. The black square shows the new possible position of one vortex point. Since the *U*-points preserve their positions the shifted vortex points must change their internal geometry (part **V**) and at the *U*-points (except the point *P*) no vortex points are located. Part **IV**, shows the possible new situation in the chosen *U*-point S.

change their internal geometry, because the *U*-points of waves *A*, *B*, *C* preserve their positions. That means that except the point *P* the internal geometry of vortex points has changed. This is an outline of the proof of two facts:

– having the four waves of constant amplitude the different vortex lattices can be generated; the vortex lattice geometry, typically, depends on the wave vector coordinates and relative phases between interfering waves;

– within the same vortex lattice generated by the four waves the vortex points may differ in their internal geometry.

Using the generalized first property this proof can be extended to more than four wave case. This proves that first property is truly special and limited to the three wave case.

The first special property results in the following fact: the distribution of vortex points within the given sublattice depends on the coordinates of wavevectors only. This fact will be called the second special property.

The second special properties can be deduced from the formulas (10)–(12), which are free of amplitudes and initial phases. To see it more clearly let us assume that one vortex point lies at the origin of the coordinates system and the wave *A* initial phase is zero ($\delta_A = 0$). Then:

$$\delta_A - \delta_B + \pi - \gamma_{AB} = 0 \tag{17a}$$

$$\delta_A - \delta_C + \pi + \gamma_{AC} = 0 \tag{17b}$$

$$\delta_B - \delta_C + \gamma_{AB} + \gamma_{AC} = 0 \tag{17c}$$

and formula (9a) become

$$xP = 2\pi \frac{lk_{yC} + mk_{yB} + (m-l)k_{yA}}{k'_{xB}k_{yC} - k'_{xC}k_{yB} + k_{xCB}k_{yA}} \tag{18a}$$

Consequently, the formula (8) becomes

$$yP = 2\pi \left[\frac{-k'_{xB}}{k'_{yB}} \frac{lk_{yC} + mk_{yB} + (m-l)k_{yA}}{k'_{xB}k_{yC} - k'_{xC}k_{yB} + k_{xCB}k_{yA}} + \frac{l}{k'_{yB}} \right] \tag{18b}$$

The same could be done for the negative case. Formulas (18) are explicit free of wave amplitude and initial phases. More physical understanding is as follows. According to the first property at every vortex point of the given sublattice there is the same triangle formed by phasors. Hence, the same CALs must go through vortex points. But the periodicity of CALs, by definition, does not depend on the wave amplitude; consequently, the distribution of vortex points within the given vortex sublattice is independent of the wave amplitude. Unfortunately, the conclusion that when the plane wave amplitude is non-uniform the vortex sublattice geometry is preserved is false. The changes in the amplitude distribution over the given plane wave shift the position of the whole vortex lattice. One can think of a plane wave that has two areas of different amplitudes. The geometrical relations between vortex points inside the interference region corresponding to each of these areas are the same, but there is additional shift between the areas. Nevertheless, the above fact can be still used to determine the vortex lattice distortion caused by the amplitude non-uniformity.

The third special property of the OVI field is: the vortex lattice geometry does not depend on the initial phases of the interfering waves. Again, typically this is not true for the case of more than three waves and can be proved by using a similar methodology as for the previous statements. While changing the phase of one, two or three waves the vortex lattice moves as a rigid body.

The ends of three wavevectors; if they are not collinear as assumed in the case of OVI, define uniquely a plane named OVI-plane, which typically, is not true in the case of four or more waves [6, 8]. This fact is the fourth special property.

The fourth special property can be proved in the following way: let us assume that the *z*-axis of the coordinate system is perpendicular to the OVI-plane. In such a coordinate system the *z*-coordinates of the three wave vectors are the same. Thus going along the lines parallel to the *z*-axis the phases of interfering waves are changing

at the same speed and the vortices must propagate along such lines. The trajectories of vortex points are described by the formulas [6, 7]:

$$\Delta x = \frac{k'_{zC}k'_{yB} - k'_{yC}k'_{zB}}{k'_{xB}k'_{yC} - k'_{xC}k'_{yB}}\Delta z \tag{19a}$$

$$\Delta y = \frac{k'_{zB}k'_{xC} - k'_{xB}k'_{zC}}{k'_{xB}k'_{yC} - k'_{xC}k'_{yB}}\Delta z \tag{19b}$$

where Δz is the shift of vortex points along the z-axis and Δx, Δy are the shifts of vortex points in xy-plane to be determined. If the z-axis is perpendicular to the OVI-plane, then $\Delta x = \Delta y = 0$.

The trajectories of vortex points are more complicated in the case of more than three plane waves.

The special properties described above allow for direct separation of the influence of wave parameters on the behavior of vortex points. As has been shown the vortex sublattice geometry depends on the coordinates of wavevectors only. The relative phase of the interfering waves has influence on the vortex lattice position (as a rigid body). The vortex amplitudes have influence on the shift between two vortex sublattices. Additionally, the dynamics of vortex points can be clearly defined in the 3-D space. Apart from these important facts there are some other relations, less general, but useful in the analysis of experimental data obtained with OVI. These relations may be easily proved using the definitions and formulas given in this paper. Four of these relations are listed below.

1. CAL period. As was mentioned above the period T of CALs, in the case of plane waves of uniform amplitude is equal to the fringe period of the interference pattern of the corresponding waves and can be calculated from the formula:

$$T = \frac{2\pi}{\left|M_x k_{xCB} + M_y k_{yCB}\right|} \tag{20}$$

It is easy to show (using the smart coordinate system) that when the denominator in expression (20) is equal zero, then both waves have the same phase difference over the whole observation plane and no vortex lattice can be identified.

2. The triangle period. While moving along the given CAL of waves B and C, which passes through vortex points phasors **b** and **c** rotate at the same angular speed. The triangle period Δ_T is a distance along which both vectors rotate through a full angle

$$\Delta_T = \frac{2\pi}{\left|K_x k_{xB} + K_y k_{yB}\right|} \tag{21}$$

3. The distance between vortices along the CAL. The distance Δ between neighboring vortex points can be determined, while moving along the CAL, which goes through vortex points

$$\Delta = \frac{2\pi}{|K_x k'_{xB} + K_y k'_{yB}|} \tag{22}$$

4. The basic cell geometry. The parallel CALs form quadrilateral cells, whose vertices are occupied by neighboring vortex points of the same topological charge (Fig. 7). These are named basic cells. Since there are three different pairs of CALs one can identify three groups of basic cells. Formula (22) allows calculating the length of cell sides. Having the vectors **K** for each CAL one can determine cell angles. In this way, the geometry of cells belonging to these three groups can be fully determined. The change of wave parameters results in changes of cell geometry and (or) the distance between vortex sublattices. These changes can be measured using OVI and allow for precise interferometric measurements.

The first, third and fourth special properties as identified above are also valid in the case of three non-plane waves of non-uniform amplitude. In the case of the fourth special property the OVI-plane must be replaced by OVI-surface and the vortex trajectories become more complex. The formulas (20)–(22) are not strictly valid when the interference waves are disturbed as it is in the case of experiment. However, real waves can be almost plane and the deflections of vortex positions may be less than three pixels of the CCD camera. In such a case all the formulas derived are of

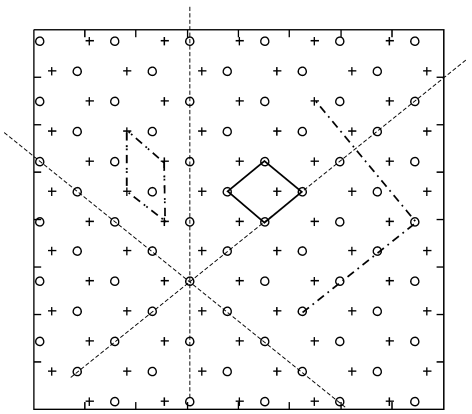

Fig. 7. The vortex lattice consists of two sublattices which are marked by pluses and circles. The CALs of wave pairs *A* and *B*, *B* and *C*, *A* and *C* are marked by dashed lines and are parallel to the corresponding two beam fringe systems. The figure shows an example of two cells whose sides are determined by CALs and one triplet. The cells vertex must be occupied by the vortex points having the same topological charge, while the triplets can be composed of any three vortex points.

practical meaning, which is shown by the experimental tests. Moreover, these effects can be easily identified and special correction procedures can be applied to improve the system resolution. In the next section, some experimental data are presented. They are analyzed by most basic procedures without any additional corrections and illustrate great possibilities of the OVI.

4. OVI applications

Two methods of data analysis are available at the moment. One is based on vortex triplet analysis (Fig. 7). The second is based on cell geometry analysis (Fig. 7). The triplet method is more complicated and accurate and can be used for both full field and point-wise measurements. The cell method is faster and simpler, but less accurate and its usefulness for point-wise measurements is limited. Both methods compare the geometry of triplets/cells before and after wave disturbance.

The OVI were tested with wave tilt measurement. In the experiment, the wave tilt was forced by optical wedge of known angle, which was inserted into one of the OVI beams (object beam) – Fig. 1. According to the manufacturer's data the angle of the wedge was 6 seconds of arc with accuracy of 1.5 second of arc. A series of measurements have shown that OVI reproduced the angle within the error given by manufacturer. These measurements have proved also that the vortex point localization procedures work in an expected way.

Placing the wedge into the object wave decreases the wave amplitude, which lowers the measurement accuracy. However, using the special properties of the OVI interference field the reference waves can be arranged in such a way that the vortex shift caused by the wave tilt and amplitude decrease are mutually perpendicular, so this error is practically eliminated.

The measured wave tilt can be decomposed into two axes perpendicular to the observation plane. Thus the orientation of the tilt axis can be determined. The same can be done by analyzing two two-beam interferograms $A + B$ and $A + C$; however this method is evidently less accurate and requires two interferograms, instead of one: $A + B + C$. The linear vibrations of the wedge do not lower the measurement accuracy. The measurements are reported in [11, 12] and the theory is described in [6, 10].

The measurements reported show the main advantage of the OVI. Instead of extracting the fringe maxima or minima, the vortex points are traced. The vortex points are stable and point-like structure, which can be located with high accuracy. Their dynamics bring more information on the evolution of wavefronts than fringe pattern and due to special properties of vortex lattice can be easily related to wavefront geometry.

When rotating the wedge through a small angle, the additional tilt of the object wave in the range of a few tens of milliseconds of arc can be precisely applied. In the case described the wedge rotation by ten degrees of arc results in the wave tilt by 70 milliseconds of arc. It was shown that the OVI can sense the rotations as small as 30 milliseconds of arc [11, 12] – Fig. 8. The diameter of active area (area

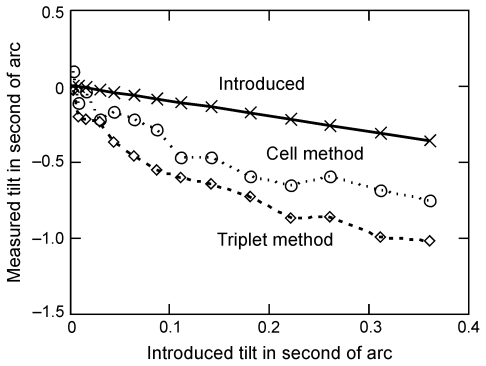

Fig. 8. The sub-millisecond wave tilt is introduced by the rotation of the optical wedge and the measured angle is an angle determined by the OVI. The bold (crosses) line shows an ideal measurement (we know the results because the tilt was precisely induced), dotted line (circles) shows the values obtained by cells method and dashed line shows values obtained by the triplet method. The OVI can sense very small angle changes, but the present data processing methods work well at the level of 0.7 second of arc. Some better data analysis methods are under investigation.

of measurement) was about 5 mm. However, more sophisticated data processing methodology is necessary to compute such small angles, which will be the subject of separate paper.

The fourth property is a base for the concept of 3-D scanning interferometry. While shifting the observation plane (the CCD camera, for example) along the vortex point propagation lines the vortex points should stay at their positions (in the observation plane). The measured disturbances of the vortex positions can be used for high resolution wavefront reconstruction. At present, this is a theoretical suggestion, which has not been tested experimentally yet.

5. Conclusions

OVI should not be considered as a single interferometer. In fact, it is a new family of interferometers, which can be developed in various directions. The OVI can be set up in many configurations. Its basic optical body can also be enhanced in as many ways as classical two beam interferometers. The number of possible measurement methodologies is even bigger than in the two beam interferometry. The OVI can be used as three two-beams interferometers. In such a case the measurements obtained by these interferometers can be mutually related at vortex points, however, this approach does not exploit all the special properties of OVI. To make full use of the OVI advantages the three beam routines should be used, as described above. There are various possibilities in this case. One of the beams can be treated as an object beam but for some measurements it is also reasonable to disturb two beams or all three beams. Also, the four-waves routine shortly mentioned in [6, 8] seems to be promising for some goals. With the OVI the measurements can be performed in both point-wise and

full field mode. The relations between vortex points within the measurement area are strong. It seems that the full field mode has deeper meaning in the case of OVI than for the classical two beam interferometer. The practical meaning of this fact is studied now. The OVI as presented above works in the simplest setup with basic methodology of measurement and data processing. In particular, the vortex point localization procedures are new and remarkable progress is still possible. Nevertheless, at this stage the OVI can compete in the field of chosen measurement with well known interferometric systems. The author expects that by improving these basic methods and developing new ones, like combining the OVI with phase shifting technique, for example [33], the OVI performance can be remarkably better.

Acknowledgments – This work was supported by the Polish Ministry of Scientific Research and Information Technology under Grant No. 3T10C04829.

References

[1] SOSKIN M.S., VASNETSOV M.V., *Singular optics*, [In] *Progress in Optics*, [Ed.] E. Wolf, Vol. 42, North-Holand, Amstredam 2001, pp. 219–76.
[2] VASNETSOV M., STALIUNAS K. [Eds.], *Optical Vortices*, Nova Science, New York 1999.
[3] ALLEN L., PADGETT M.J., BABIKER M., *The orbital angular momentum of light*, [In] *Progress in Optics*, [Ed.] E. Wolf, Elsevier Science B.V., New York, Vol. 39, 1999, pp. 291–372.
[4] ABRAMOCHKIN E.G., LOSEVSKY N., VOLOSTNIKOV V., *Generation of spiral-type laser beams*, Optics Communications **141**(1–2), 1997, pp. 59–64.
[5] ANGELSKY O.V., BESAHA R.N., MOKHUN I.I., *Appearance of wave front dislocations under interference among beams with simple wave fronts*, Optica Applicata **27**(4), 1997, pp. 273–8.
[6] MASAJADA J., *Optical Vortices and their Application to Interferometry*, Oficyna Wydawnicza Politechniki Wrocławskiej, Wrocław 2004 (monographs of Wrocław University of Technology).
[7] MASAJADA J., DUBIK B., *Optical vortex generation by three plane wave interference*, Optics Communications **198**(1–3), 2001, pp. 21–7.
[8] MASAJADA J., POPIOŁEK-MASAJADA A., WIELICZKA D., *The interferometric system using optical vortices as phase markers*, Optics Communications **207**(1–6), 2002, pp. 85–93.
[9] MASAJADA J., POPIOŁEK-MASAJADA A., FRĄCZEK E., FRĄCZEK W., *Vortex points localization problem in optical vortices interferometry*, Optics Communications **234**(1–6), 2004, pp. 23–8.
[10] MASAJADA J., *Small-angle rotations measurement using optical vortex interferometer*, Optics Communications **239**(4–6), 2004, pp. 373–81.
[11] POPIOŁEK-MASAJADA A., BORWIŃSKA M., DUBIK B., *Testing a new method for small-angle rotation measurements*, Proceedings of SPIE **5858**, 2005, pp. 195–201.
[12] POPIOŁEK-MASAJADA A., BORWISKA M., FRĄCZEK W., *Testing a new method for small-angle rotation measurements with the optical vortex interferometer*, Measurement Science and Technology **17**(4), 2006, pp. 653–8.
[13] FRĄCZEK E., FRĄCZEK W., MROCZKA J., *Experimental method for topological charge determination of optical vortices in a regular net*, Optical Engineering **44**(2), 2005, p. 025601.
[14] FRĄCZEK E., FRĄCZEK W., MASAJADA J., *The new method of topological charge determination of optical vortices in the interference field of the optical vortex interferometer*, Optik – International Journal for Light and Electron Optics **117**(6), 2006, pp. 423–5.
[15] FRĄCZEK E., FRĄCZEK W., *Two methods to determine topological charge in regular net of optical vortices*, Proceedings of SPIE **5858**, 2005, pp. 247–53.

[16] GHIGLIA D.C., PRITT M.D., *Two-Dimensional Phase Unwrapping: Theory, Algorithms, Software*, Wiley 1998.
[17] MALACARA D., MALACARA Z., SERVIN M., MALCACARA Z., *Interferogram Analysis for Optical Testing*, Dekker/CRC Press, 2005.
[18] FRANCON M., *Optical Interferometry*, Academic Press, New York 1966.
[19] NICHOLLS K.W., NYE J.F., *Three-beam model for studying dislocations in wave pulses*, Journal of Physics A: Mathematical and General **20**(14), 1987, pp. 4673–96.
[20] BIALYNICKI-BIRULA I., BIALYNICKA-BIRULA Z., *Vortex lines of the electromagnetic field*, Physical Review A **67**(6), 2003, p. 062114.
[21] SCHONBRUN E., PIESTUN R., JORDAN P., COOPER J., WULFF K.D., COURTIAL J., PADGETT M., *3D interferometric optical tweezers using a single spatial light modulator*, Optics Express **13**(10), 2005, pp. 3777–86.
[22] PRIMOT J., *Three-wave lateral shearing interfermometer*, Applied Optics **32**(31), 1993, pp. 6242–9.
[23] PRIMOT J., SOGNO L., *Achromatic three-wave (or more) lateral shearing interferometer*, Journal of the Optical Society of America A **12**(12), 1995, pp. 2679–85.
[24] DARLIN J.S, SENTHILKUMARAN P., BHATTACHARYA S., KOTHIYAL M.P., SIROHI R.S., *Fabrication of an array illuminator using tandem Michelson interferometers*, Optics Communications **123**(1–3), 1996, pp. 1–4.
[25] GUÉRINEAU N., PRIMOT J., *Nondiffracting array generation using an N-wave interferometer*, Journal of the Optical Society of America A **16**(2), 1999, pp. 293–8.
[26] VELGHE S., J. PRIMOT J., GUÉRINEAU N., COHEN M., WATTELLIER B., *Wave-front reconstruction from multidirectional phase derivatives generated by multilateral shearing interferometers*, Optics Letters **30**(3), 2005, pp. 245–7.
[27] PATRA A. S., KHARE A., *Interferometric array generation*, Optics and Laser Technology **38**(1), 2006, pp. 37–45.
[28] HUTLEY M.C., *Optical techniques for the generation of microlens arrays*, Journal of Modern Optics **37**(2), 1990, pp. 253–65.
[29] MAO W., ZHONG Y., DONG J., WANG H., *Crystallography of two-dimensional photonic lattices formed by holography of three noncoplanar beams*, Journal of the Optical Society of America B **22**(5), 2005, pp. 1085–91.
[30] FRIED D.L., VAUGHN J.L., *Branch cuts in the phase function*, Applied Optics **31**(15), 1992, pp. 2865–82.
[31] FRIED D.L., *Adaptive optics wave function reconstruction and phase unwrapping when branch points are present*, Optics Communications **200**(1–6), 2001, pp. 43–72.
[32] FREUND I., SHVARTSMAN N., *Wave-field phase singularities: The sign principle*, Physical Review A **50**(6), 1994, pp. 5164–72.
[33] MASAJADA J., *The internal scanning method with optical vortex interferometer*, Proceedings of SPIE **5958**, 2005, pp. 433–41.

Received March 29, 2006
in revised form November 21, 2006